



HAL
open science

Transient-TLP (T-TLP): a simple method for accurate ESD protection transient behavior measurement

David Trémouilles, Antoine Delmas, Nicolas Mauran, Nicolas Nolhier,
Houssam Arbess, Marise Baffleur

► **To cite this version:**

David Trémouilles, Antoine Delmas, Nicolas Mauran, Nicolas Nolhier, Houssam Arbess, et al.. Transient-TLP (T-TLP): a simple method for accurate ESD protection transient behavior measurement. EOS/ESD Symposium, Sep 2013, LAS VEGAS, United States. pp.258-267. hal-01056511

HAL Id: hal-01056511

<https://hal.science/hal-01056511>

Submitted on 20 Aug 2014

HAL is a multi-disciplinary open access archive for the deposit and dissemination of scientific research documents, whether they are published or not. The documents may come from teaching and research institutions in France or abroad, or from public or private research centers.

L'archive ouverte pluridisciplinaire **HAL**, est destinée au dépôt et à la diffusion de documents scientifiques de niveau recherche, publiés ou non, émanant des établissements d'enseignement et de recherche français ou étrangers, des laboratoires publics ou privés.

Transient-TLP (T-TLP): a simple method for accurate ESD protection transient behavior measurement.

David Trémouilles (1,2), Antoine Delmas (3), Nicolas Mauran (1,2), Nicolas Nolhier (1,4), Houssam Arbess (1,2), Marise Bafleur (1,2)

(1) CNRS, LAAS, 7 Avenue du Colonel Roche, F-31400 Toulouse, France
e-mail: david.tremouilles@laas.fr

(2) Univ de Toulouse, LAAS, F-31400 Toulouse, France

(3) Freescale Semiconductor Inc.; AISG-AMPD; 134 avenue du Général Eisenhower, 31023 Toulouse, France,
now with : ST Microelectronics, 850, rue J.Monnet, BP. 16, 38926 Crolles, France

(4) Univ de Toulouse, UPS, LAAS, F-31400 Toulouse, France

Abstract – Understanding the transient behavior of ESD protection devices is a key to optimize IC protection solutions. However, outside of the ESD world, electrical characterization of pulsed electrical signal involving both kilowatts of power and extreme frequency bandwidth (DC to several GHz) is definitely not common. Dedicated and specific measurement methodologies are thus required. In this work, we proposed a new and simple method that allows accurate triggering behavior measurements based on a standard very-fast TLP setup, which does not compromise on any performance aspects (bandwidth, maximum current, single-pulse, simplicity...) and does not require any additional or external characterization equipment.

Introduction

Transient analysis of protection devices during an ElectroStatic Discharge (ESD) has been demonstrated to be very important to improve and optimize IC robustness and not only for triggering behavior [1,2].

ESD electrical conditions are extreme and quite specific. They consist in a combination of very high-power electrical stress having a wide frequency bandwidth (on the order of kW's and from DC up to GHz's). Moreover, most protection devices present a highly non-linear characteristic, which is directly related to their switching behavior. Electrical characterization of kW-power and broadband signal is not common outside of ESD world therefore dedicated and original measurement setups are required.

We have developed and demonstrated a new and simple setup to characterize transient electrical behavior of ESD protection devices with high accuracy. Only what is already available around a typical Transmission Line Pulse (TLP) tester is needed. Specific high frequency characterization tools are *not required* in contrast to our previously presented setup [4].

The first section of this paper is a review of the different approaches already published. The second section summarizes our previous work and demonstrates the new methodology. In the last section a measurement example is shown.

I. A Review of Published Measurement Methods

Using TLP for ESD device characterization has almost thirty years of history. In the next subsection we will give a summary of the major steps that brought us to today's ESD transient measurement solutions based on TLP. In the second section we will propose a rough classification of the available methods and summarize their main advantages and drawbacks.

A. A bit of history on using TLP for transient measurement.

The publication of T. Maloney in 1985 gave birth to TLP as the reference characterization technique to gather information on ESD devices behavior [3].

Almost ten years later, in 1996, H. Gieser demonstrated Very Fast TLP (VF-TLP), which is a refinement of the TLP concept that allows measuring

with very narrow pulses, shorter than 10 ns, compared to the typical 100ns pulses of a more classical TLP tester [5]. While classical TLP testers were designed to approximately match Human Body Model (HBM) ESD stress in terms of waveform characteristics (rise-time, duration) and total dissipated energy, VF-TLP was proposed to match better with Charged Device Model (CDM) ESD stresses. Furthermore, in the work of H. Gieser a simple method to reconstruct both voltage and current transient at the Device Under Test (DUT) is proposed. The proposed transient measurement concept was successfully and well illustrated some years later in 2003 in [6] and in 2004 in [7].

Almost twenty years after the T. Maloney publication, and about ten years after the H. Gieser one, the first two papers using a classical TLP setup to obtain ESD device transient information were published. Most importantly they started the careful consideration regarding how the TLP tester parasitics affected the transient measurement results and how the distortion could be reduced. First, in April 2005, R. Ashton presented a method [8] that used the measured current and voltage waveforms from a classical TLP setup to extract incident and reflected pulses and to recombine these two pulses after shifting them appropriately in time to obtain the voltage at the DUT. He further improved the method by considering how to characterize and de-embed the serial resistance and inductance essentially brought by the probe needles. In September of the same year, D. Trémouilles proposed a slightly more advanced method that in addition takes into account frequency dependent attenuation of the cables [9]. This method is based on a rather simple model of the TLP testers, whose parameters are extracted by a Vector Network Analyzer (VNA) measurement of some tester parts.

In 2006, H. Wolf demonstrated a VF-TLP setup dedicated to transient measurement [10] based on Gieser's work twenty years before. In contrast to the standard VF-TLP setup it requires a solid-state pulse generator and a sampling scope and uses many successive pulses to obtain one waveform. One year later, J.R. Manouvrier also proposed a very similar setup [11].

In 2007, the excellent "Survey on Very Fast TLP and Ultra Fast Repetitive Pulsing for Characterization in the CDM-Domain" by H. Gieser summarized the advances on that type of work [12].

The most productive year regarding TLP transient analysis is certainly 2009. The most important aspect is that for the first time the influence and potential distortions of the voltage and current probes

themselves have been taken into account and some corrective actions to limit their impact on the transient waveforms have been used. The most advanced and impressive characterization work on a TLP system and its use to correct measured waveform was proposed by R. Gillon [13]. A full RF-characterization of the setup was carried out using advanced RF equipment. All possible parasitics from the scope to the DUT are characterized and taken into account in the calculation of the actual voltage and current at the DUT from the current and voltage waveform measured on the oscilloscope. A. Delmas demonstrated an equivalent but much simple solution that only, but still, required using a VNA [4]. This method also allows including corrections for the voltage probe, which is the only correction required in this VF-TLP setup (a current probe is not used) and also includes correction for cables frequency dependent losses. Finally, D. Linten demonstrated a method to obtain transient information from a standard VF-TLP setup, which does not require any "exotic" generator or VNA, but it does not take into account any kind of losses in the cables nor any attenuation introduced by current or voltage probes [14]. However, it takes into account the parasitic resistance and inductance from the non-RF wafer probes used in this setup.

B. Advantages and limitations of the main solutions

As we saw in the previous section, many different approaches have been implemented to measure the transient behavior of ESD protection devices over the last twenty years. We propose here a classification to underline their advantages and limitations.

First, it must be stated that there is no hope to measure faster transient than the TLP oscilloscope can properly measure. The oscilloscope used is the first limitation that should be considered.

It should also be noted that all methods require some amount of signal processing to align incident and reflected pulses in time and sum them to obtain the voltage at the DUT. The only method that would not require such a processing is the Kelvin measurement. However, for this configuration the time alignment of current and voltage waveforms is lost and might be difficult to recover precisely and will require signal processing. Furthermore Kelvin measurement requires using high impedance probes, which might imply limitation on the bandwidth and distortions that should be considered carefully and probably corrected for. Kelvin measurement will not be considered in this paper.

Moreover we will see that all of these methods have to make compromises on several different aspects:

- the fastest transient that can be measured,
- the maximum voltage or current that can be measured,
- the requirement of several pulses to obtain one waveform,
- the precise synchronization of current and voltage waveforms, as well as incident and reflected ones,
- the correction (or not) of attenuation induced by the current and voltage probes and/or the cables.

Let us first draw a line in between systems that requires specific equipment for the measurement itself and the one that uses the most standard/simple TLP systems.

In the first group we found the solution that led to the most publications. This is a solution based on repetitive testing that inherently requires a solid-state pulse generator and a sampling scope. This is certainly the solution that offers the highest possible bandwidth and accuracy. However, on top of requiring quite dedicated equipment (very stable pulse generator and sampling scope), it also suffers severe limitation regarding maximum possible voltage that are typically limited to 10V and might be extended to 150V with the best pulse generator that exists nowadays. This solution does not allow observing a single shot pulse as it require repeated pulses. Therefore, phenomena like avalanche breakdown delay [15] cannot be effectively studied with such a system. And finally, up to now frequency dependent attenuation of the cables was not taken into account in such solutions.

In the second group we considered solutions based on quite standard VF-TLP or TLP measurement systems. An excellent comparison of the possible variations of such systems is available in [12]. We will consider here the simplest one regarding wafer probing, which is the Time Domain Reflectometer (TDR) configuration. It requires only one wafer probe as compared to two for the other ones. We believe the usage of non-RF probes should be discouraged. Indeed non-RF probes are a very risky option that often requires too much correction level, which can severely degrade measurement accuracy. Furthermore, even if the parasitics of the wafer probes can effectively be modeled and extracted, their values depend on their geometrical placement and their environment that might be very different from the one used to extract correction parameters. As just defined, this second group can be subdivided in two

subgroups. In the first subgroup we find solutions based on modeling the system and methods to extract the model parameters [8, 9, 14], and a second subgroup, which is all measurement based using a raw S-parameter measurement technique [4, 13]. While the second subgroup is the most accurate, up to now it required a dedicated RF measurement setup. This is also the only solution that integrates correction for the voltage and/or current probes. The advantage of the first subgroup is that parameter extraction is generally possible with simple calibration steps not requiring additional measurement equipment if the model is simple enough. However, voltage and/or current probe correction seems quite difficult to integrate and was not achieved up to now. Both solutions suffer limitations; the modeling approach can be over simplified, while the correction parameter extractions can be overly complex.

The new technique presented in this paper proposes both a simple and accurate solution. It takes into account cable and probe frequency responses without requiring any additional equipment. The transient measurement is only limited by the oscilloscope and possibly by the voltage probe bandwidth but its behavior can be corrected by the method (at least partially). The maximum current and voltage are determined by VF-TLP system itself. It allows single shot measurement, with precise timing alignment fully included in the de-embedding-parameter extraction procedure.

II. New Method

The Transient TLP (T-TLP) technique we proposed here is the final achievement of several years of work carried out at LAAS-CNRS. A summary of previous work is presented in the first sub-section. It serves as foundations for the new method, which is presented in the second sub-section. In the last part, the main precautions required to carry out successful measurements are presented.

A. Summary of previous work

In our previous work we analyzed the VF-TLP setups to understand their limitations to provide accurate measurement of transient waveforms [4]. Among others, coaxial cable attenuation, filtering from voltage and current probes and delay adjustment issues to properly sum the incident and reflected waveforms were carefully considered. Based on this thorough understanding, we proposed a new methodology to measure, correct and accurately recombine measurement data.

1. Previous work setup

The drastically simplified VF-TLP setup studied in our previous work is represented in figure 1. Only the voltage probe was used to acquire transient waveforms. A RF wafer-probe was used. It introduces an 80 ps delay that requires an extra correction step.

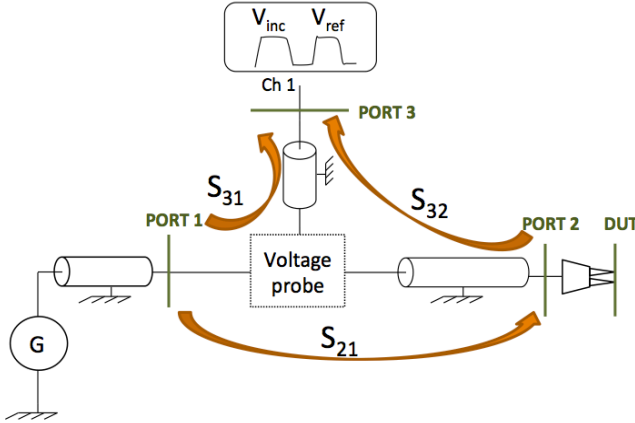


Figure 1: Schematic representation of the T-TLP setup modeled with S-parameters.

2. Summary of the previous reconstruction method

In our previous work, it has been demonstrated that voltage in PORT2 could be calculated from measured waveform using the following formula in the frequency domain:

$$V_{PORT2} = \frac{S_{21}}{S_{31}} V_{inc}^{Ch1} + \frac{1}{S_{32}} V_{ref}^{Ch1} \quad (1)$$

with V_{inc}^{Ch1} being the measured incident waveform, V_{ref}^{Ch1} the reflected one and S_{21} , S_{31} and S_{32} being scattering parameters coefficients.(Fig.1).

The three scattering parameters were measured using two Vector Network Analyzers (VNA). The first one was used for the lower frequency part from 9 kHz to 4GHz and the second for the higher frequency part from 40 MHz to 40 GHz. This calibration step, mandatory before any useful measurement, is particularly heavy and requires dedicated equipment that may not be available in most ESD laboratories.

The additional wafer probe delay was obtained from time domain measurements and treated separately. It is obtained by comparing the time delay difference between the incident and reflected pulses on an open with and without the wafer probe. This additional calibration step might be error prone.

It is important to underline the fact that incident and reflected waveforms need to be computed separately. As a consequence, it is critical to have a sufficient separation between them.

With all calculations being carried out in frequency domain, measured waveforms have to be transformed using classical Fast Fourier Transforms (FFT). At the end of the calculation, inverse Fourier transforms are used to switch back to time domain.

B. The new methodology

The new methodology presented in this section was originally proposed and developed by D. Trémouilles and A. Delmas within the framework of A. Delmas' PhD thesis [16]. The underlying mathematical processing is presented here in a new and more systematic way with regards to the PhD work.

We will show in this section that all calibration parameters can actually be obtained using the TLP setup alone, without requiring dedicated test equipment. Furthermore we will demonstrate how the additional wafer-probe time delay is self-included in the new calibration method.

Only two rather fast (a few minutes) calibration steps are actually required and are done **once and for all** at the beginning of the measurement session. The first step consists in measuring directly the incident pulse using the second channel of the oscilloscope. The second calibration is a "classical" short-load measurement.

The two calibration steps of this new method can be compared to "standard" TLP (quasi-static) open and short calibration. They serve similar purposes but extend to the time domain requirements.

The method is based on the same equation (1) as the previous one. This equation gives the voltage at PORT2 given the measurement of the incident and reflected waveforms. To effectively use this equation it is required to determine several S-parameters of the measurement setup. The S-parameters were measured with a VNA in the previous work. It is demonstrated in this work that they can also be obtained through time domain measurements using only the raw TLP setup, with only two quick calibration steps.

Before describing the two calibration steps we will first describe hereafter how to include the additional wafer-probe delay contribution. We use the previous work expression of the voltage at PORT2 to derivate the voltage at the DUT (Fig.1). We assume here that the RF probes only introduce a time delay, and that given their small length and wideband performance they introduce negligible attenuation.

In the right-hand side of equation (1), the first term of the sum is actually the incident waveform at PORT2 and the second term is the reflected one at the same port. Both incident and reflected waveforms are

related to the waveform measured on the scope through the S-parameters calculations.

The time shift introduced by the wafer-probes applies in opposite directions on the incident and reflected pulses. The incident waveform reaches the DUT slightly after PORT2. On the contrary, the reflected waveform is created by the DUT slightly before it reaches PORT2 (Fig.1). Therefore we have to move the incident waveform forward while moving the reflected one backward. This corresponds to opposite phase shifts (Φ_p) of incident and reflected waveforms in the frequency domain. In a mathematical form, this translates into:

$$V_{DUT} = \frac{S_{21}}{S_{31}} V_{inc}^{Ch1} e^{j\Phi_p} + \frac{1}{S_{32}} V_{ref}^{Ch1} e^{-j\Phi_p} \quad (2)$$

The required initial equations (1) and (2) being established, the two calibration steps and the final reconstruction of the voltage are described in the following three sections.

1. Direct pulse measurement calibration

For the first calibration step, the second channel of the oscilloscope is used to directly measure the incident pulse through a large value and high bandwidth attenuator (Fig.2). PORT2, as defined in figure 1, is thus connected to an attenuator placed directly at the second input channel of the scope. Therefore, the direct pulse incident waveform ($V_{inc, direct}$) is measured through the voltage probe on scope channel one (Ch1 or PORT3) and simultaneously and directly on scope channel two (Ch2) through the attenuator.

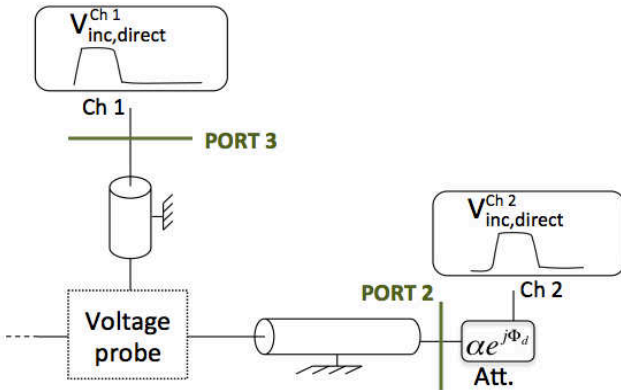


Figure 2: schematic representation of the setup for direct pulse measurement calibration step.

The attenuator obviously introduces an attenuation value α (equal to 100 for instance), which is defined by the factor by which the signal is divided. In addition the attenuator introduces a time delay on the direct signal (Fig.2). This delay translates into a phase shift (Φ_d) in the frequency domain. Thus:

$$V_{inc,direct}^{P2} = V_{inc,direct}^{Ch2} \alpha e^{j\Phi_d}$$

From equation (1) and as there is no reflected pulse on the 50Ω inputs of the oscilloscope:

$$V_{inc,direct}^{Ch2} \alpha e^{j\Phi_d} = \frac{S_{21}}{S_{31}} V_{inc,direct}^{Ch1}$$

We finally obtain:

$$\frac{S_{21}}{S_{31}} = C_1 e^{j\Phi_d} \quad (3),$$

with C_1 being a factor obtained from the scope's Ch1 and Ch2 measurement data. Knowing the selected attenuator value α we have:

$$C_1 = \frac{\alpha V_{inc,direct}^{Ch2}}{V_{inc,direct}^{Ch1}}$$

2. Short measurement with installed wafer-probe

The probe needles are installed and shorted by probing on a metallic surface (Fig.3).

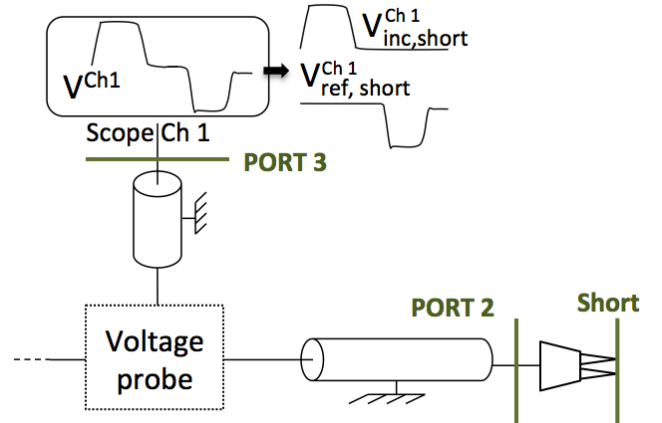


Figure 3: schematic representation of the setup for short measurement calibration step.

The voltage is zero when the DUT is a short, therefore using equation (2) we obtain:

$$\frac{1}{S_{32}} V_{ref,short}^{Ch1} e^{-j\Phi_p} = -\frac{S_{21}}{S_{31}} V_{inc,short}^{Ch1} e^{j\Phi_p}$$

and finally:

$$\frac{1}{S_{32}} = C_2 \frac{S_{21}}{S_{31}} e^{j2\Phi_p} \quad (4)$$

With C_2 directly calculated from measurements on the short circuit:

$$C_2 = -\frac{V_{inc,short}^{Ch1}}{V_{ref,short}^{Ch1}}$$

In order to double-check another equivalent coefficient might also be obtain using an open measurement following the same reasoning as for the short measurement:

$$C_2^{open} = \frac{V_{inc,open}^{Ch1}}{V_{ref,open}^{Ch1}}$$

Using either C_2 obtained with the short or open measurement gives very similar result. The probe contact resistance alone is relatively small and all other serial resistances in the setup are being taken into account by the method. It can be mathematically demonstrated that this resistance introduces a systematic below-one-percent error at each measurement point and that this error can be rigorously compensated for. The mathematical development and the corresponding correction method might be the topic of a future paper. Overall, our experiments show that most of the time the probe contact resistance alone does not significantly impact the measurement results and that it can be neglected, at least at a first sight. Carrying out reconstruction calculations with both coefficients obtained from short and open measurement allows evaluating the amount of error made by neglecting the probe contact resistance.

3. Reconstruction of DUT voltage and current

From the two previous calibration measurements, “direct pulse” and “short”, we have calculated two factors C_1 and C_2 . We will now show how to use them to correct a DUT measurement.

Doing quite simple algebra starting from equations (2), by successive substitutions we first introduce C_2 factor using equation (4):

$$V_{DUT} = \frac{S_{21}}{S_{31}} V_{inc}^{Ch1} e^{j\Phi_p} + C_2 \frac{S_{21}}{S_{31}} e^{j2\Phi_p} V_{ref}^{Ch1} e^{-j\Phi_p}$$

$$V_{DUT} = \frac{S_{21}}{S_{31}} (V_{inc}^{Ch1} e^{j\Phi_p} + C_2 e^{j\Phi_p} V_{ref}^{Ch1})$$

and finally:

$$V_{DUT} = \frac{S_{21}}{S_{31}} e^{j\Phi_p} (V_{inc}^{Ch1} + C_2 V_{ref}^{Ch1})$$

then we introduce C_1 using equation (3):

$$V_{DUT} = C_1 e^{j\Phi_d} e^{j\Phi_p} (V_{inc}^{Ch1} + C_2 V_{ref}^{Ch1})$$

We finally obtain:

$$C_1 (V_{inc}^{Ch1} + C_2 V_{ref}^{Ch1}) = V_{DUT} e^{-j(\Phi_d + \Phi_p)}$$

Which means that from C_1 , C_2 coefficients and from the incident and reflected waveforms, we obtain the

voltage at the DUT shifted by an unknown time delay. This unknown delay is not critical at all. Indeed, it just shifts the whole voltage waveform in time without modifying its shape. In other words, it only changes the time origin, which is not important in our case. Finally, all the required information about transient behavior is fully obtained by using the expression:

$$V_{DUT} = C_1 (V_{inc}^{Ch1} + C_2 V_{ref}^{Ch1})$$

All required corrections (voltage probe linearity, cables delays and attenuations and wafer-probes delays) are fully included in the two factors obtained from the two simple calibration steps.

The current at the DUT is directly obtained with the same method:

$$I_{DUT} = \frac{1}{Z_c} C_1 (V_{inc}^{Ch1} - C_2 V_{ref}^{Ch1})$$

with Z_c the characteristic impedance of the transmission lines (usually 50 Ω) and C_1 and C_2 the same coefficients as for the voltage calculation.

C. Precautions required for successful measurement

The practical manipulations to obtain the two calibration coefficients as well as the waveform for a device are pretty straightforward and do not require more care than “standard” TLP calibration steps.

It should be noticed that the scope bandwidth is a strong limiting factor. If the incident pulse is too fast to be measured by the oscilloscope there is no way to obtain accurate transient information for any device. One must make sure that the rise time of the incident pulse is lower than the intrinsic rise time of the oscilloscope.

The main precautions that need to be taken into account are more related to data mathematical post-processing. Indeed, a perfect separation of incident and reflected pulses is required. Therefore, a sufficiently long cable in between the voltage probe and the DUT (Figure 1) must be used for the reflected pulse to be ‘far’ enough from the incident one on the scope screen. Any residual incident pulse added to the rising part of the reflected one would alter triggering behavior measurement. In addition, to better separate incident and reflected pulses, an additional measurement can be done with a matched load in PORT 2. The obtained signal is a “pure” incident signal (figure 4-b). A pure reflected signal can then be obtained by subtracting previously measured “pure” incident signal to DUT measurement (figure 4-c).

Parasitic reflections on impedance discontinuities within the test bench can also interfere with scope signal. As far as possible, the test bench must be improved so that parasitic reflections appear outside of incident and reflected pulses on the scope screen. They must then be removed from the signal before it is included in the calculation of C_1 and C_2 . Apodization functions such as “tapered cosine” windows where applied to the signal to help remove parasitics without introducing distortions (figure 4-d).

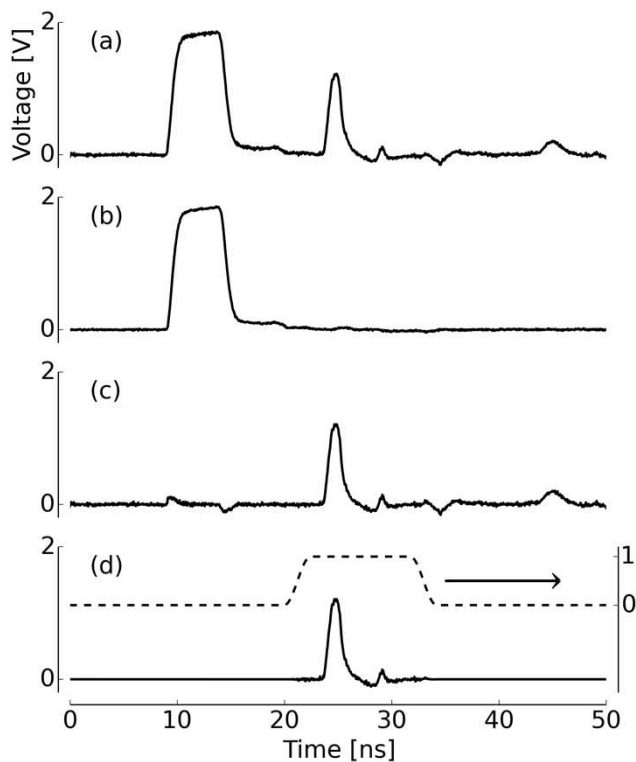


Figure 4: (a): 40 V vf-TLP raw data showing incident and reflected pulse as measured on a high voltage NPN ESD protection in a Smart Power technology. (b): “Pure” incident waveform obtained with a matched load on PORT 2. (c): “Pure” reflected waveform obtained by subtracting waveforms (b) from waveform (a). Parasitic reflections can be seen after the fall of the reflected pulse. (d): Tapered cosine window function (dashed line) used as apodization function on reflected signal. Corrected waveform is represented in solid line.

The purpose in the above example is to clean up the reflected pulse from rather low frequency components coming from the end of the incident pulse. This justifies using an averaged incident pulse measurement. The averaging attenuates high frequency components in the incident pulse, which helps to preserve the fast transient information when the incident pulse is subtracted from the measurement. However, it results that two peaks (up and down) appears at the beginning of the waveform on figure 4-

d, which are removed by the apodization operation. It is important to notice that the averaged incident pulse must only be used for the clean up operation and that the real incident pulse (from the single shot measurement) must be used for all other calculations.

Particular attention has to be paid to the calculation of C_1 and C_2 calibration coefficients. The underlying mathematical calculation actually corresponds to a deconvolution process. Calculation of such a mathematically ill-posed problem is very sensitive to noise. Therefore, a proper/intelligent filtering operation has to be done to obtain these coefficients. Nahman-Guillaume causal filters [17,18] were applied to C_1 and C_2 ratios in order to attenuate divergent values obtained when the denominator approaches zero. During the two calibration measurements, some waveform averaging using repeated pulse might be used to further reduce noise. However, this option should be implemented carefully to preserve enough high frequency information in the calculated coefficients, which is crucial to derive properly the device transient information.

III. Measurement example

To illustrate the measurement method, an example of results that can be achieved using the T-TLP method is presented in this section. The transient behavior of a high voltage ESD protection device as a function of a static voltage applied on its gate is measured.

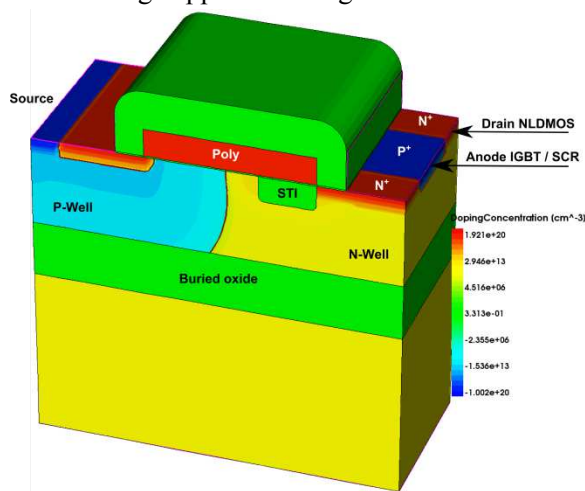


Fig. 5 : Structure of the “elementary cell” of the measured device.

The device under test combines MOS, IGBT and SCR operation in a single component and has been thoroughly studied in [19]. It is a power clamp for high-temperature operation (200°C) providing a very compact high-robustness ESD protection with low sensitivity to temperature. It is achieved by inserting in the same LDMOS device P+ diffusions in the drain (Fig.5). It was designed to replace an LDMOS-based

power clamp whose on-resistance is very sensitive to temperature. However, detrimental SCR triggering can occur with voltage overshoot. The combination with the MOS and IGBT devices is expected to limit this negative effect. Accurately characterizing this dynamic behavior is then crucial for the efficiency of the protection design.

A very stable gate biasing was obtained using an additional high frequency probe having an integrated capacitor. The stability of the bias has been monitored using a high bandwidth bias tee, which allows measuring any instability of the gate biasing on another channel of the oscilloscope.

Figure 6 shows the transient voltage and current calculated at the device with the proposed method for three different gate biases.

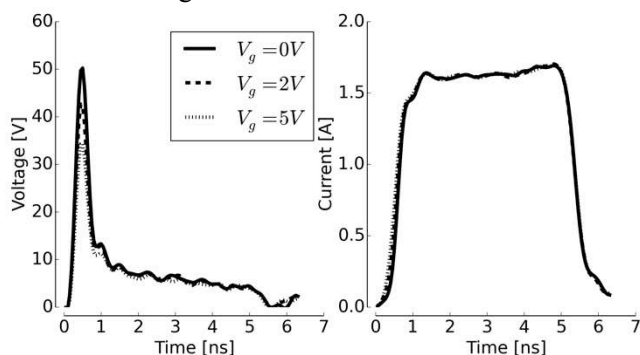


Figure 6: T-TLP measurement results showing transient voltage (left) and current (right) in the measured device for three different voltages applied to the device gate during the measurements.

The magnified view on figure 7 demonstrates that the voltage overshoot during this 1.5 A TLP pulse is significantly reduced for increasing gate voltages.

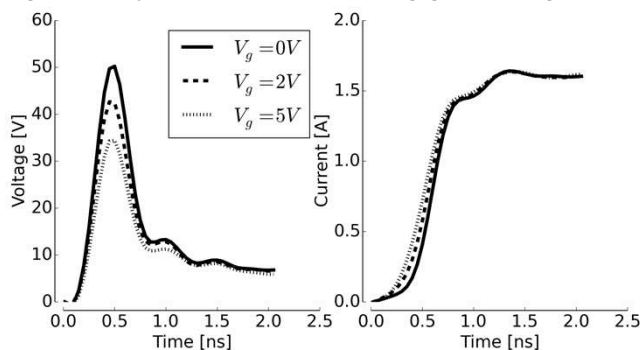


Figure 7: Magnified view of Fig.6 centered on the triggering region of the device. Triggering voltage overshoot is significantly reduced with increasing static gate bias voltage.

Using gate biasing helps limit overvoltage to safe value for gate oxide protection. Indeed, the typical gate oxide thickness of this technology is 16.5 nm that corresponds to a static breakdown voltage of 20 V. However, with the 5 V gate bias, the overvoltage is limited to 30 V maximum over less than 1 ns, which

is well below the 40 V breakdown voltage of the gate oxide measured under such short pulses [20].

By design, in the proposed method current and voltage waveform are perfectly synchronized. As a result, we can accurately plot the current vs. voltage state of the device at each time point (Fig.8). Such representation might be interesting to visualize the triggering behavior of the device. It must be noted that the TLP I(V)-like part of the curve is extremely different from the one that might be obtained with an HBM-like pulse. Indeed, the HBM I(V) curve corresponds to a relatively slow falling waveform whereas here it corresponds to the very fast falling part of the TLP pulse. Therefore while HBM I(V) has been demonstrated to match well classical TLP curves, this should definitely not be expected using the TLP transient I(V).

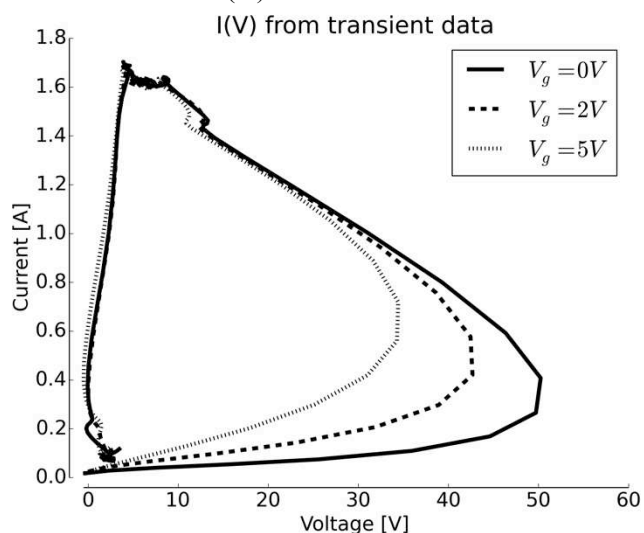


Figure 8: Current versus voltage trace using current and voltage couple extracted at each instant of the transient waveforms from figure 6.

The perfect current and voltage synchronization also allows many different investigations to better understand the device behavior during the transient.

First, we can compute the instantaneous power in the device by calculating the voltage-current product at each instant of the transient. The results show that for the same pulse amplitude the power in the device is almost independent of the gate biasing (Fig.9 left). This fact corroborates the observation that the maximum current (I_{t2}) is independent of the gate bias.

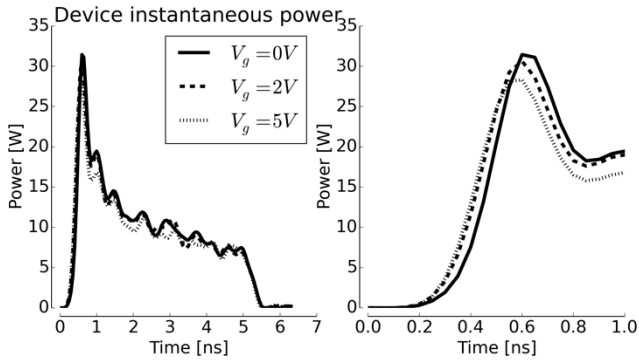


Figure 9: Instantaneous power of the device (voltage-current product) for three different gate biases, during the whole pulse (left) and magnified around the triggering region (right). The power in the device is not very significantly affected by the gate bias.

Even during the triggering the power is not significantly different as can be observed in the right graph of figure 9. Indeed while the voltage at the device is lower for higher gate bias voltages, the current delivered to the DUT is increased (Fig.7), and thus the total power in the device remains quite stable. Secondly, in contrast to the gate-bias independence of the instantaneous power in the device, the instantaneous on-resistance of the device shows the beneficial effect of the gate biasing to reduce the voltage overshoot (Fig.10). The instantaneous on-resistance is the ratio of the voltage over the current at each instant of the transient.

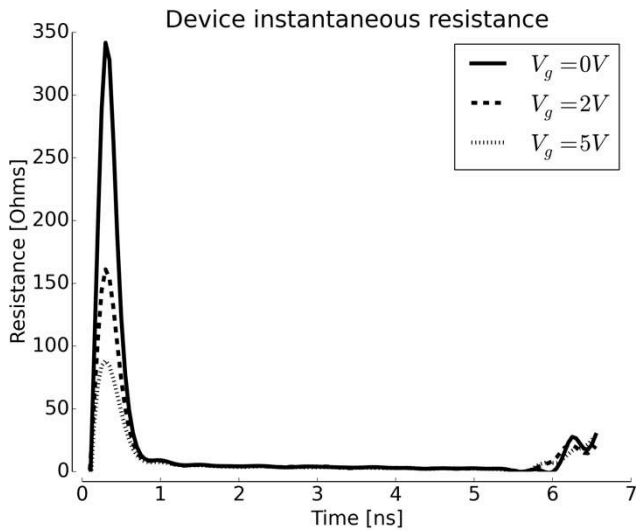


Figure 10: Instantaneous on-resistance of the device (voltage over current ratio) for the three different gate bias. Gate biasing significantly reduce the impedance of the device during triggering.

The maximum equivalent on-resistance of the DUT is almost divided by four for a gate bias of five volt as compared with the gate grounded.

It is also interesting to observe the increased equivalent resistance of the device at the end of the pulse when it turns off (Fig.10).

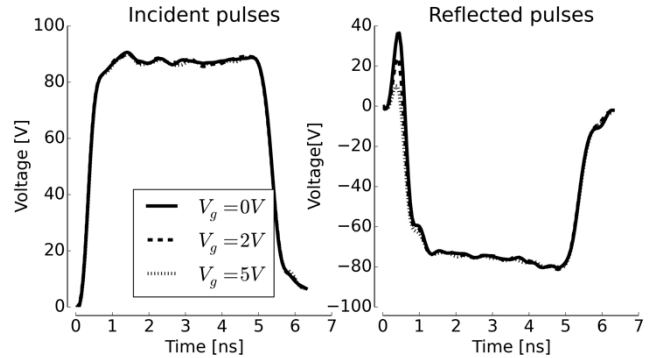


Figure 11: Incident (left) and reflected (right) pulses calculated from the voltage and current transient waveforms from fig.6. As it could be expected all the incident pulses are identical (generated by the TLP system). The entire device related information is actually contained in the reflected pulses.

Finally, the proposed method gives directly the voltage and current at the DUT. Incident and reflected pulses are never explicitly computed during the calculation. However, we still can calculate incident and reflected pulses from the obtained current and voltage waveforms in the classical and straightforward way. This allows verifying that the incident pulse is independent of the tested device or its configuration (Fig.11 left). Indeed the incident pulse is defined by the pulse generator only whereas the reflected pulse carries all device related information (Fig. 11 right).

Conclusion

The new transient analysis measurement method demonstrated in this paper is simple yet highly accurate. Only two quick calibration steps are required to fully correct for tester parasitics. No additional RF-testing equipment is necessary. A measurement example demonstrates that excellent results can be achieved and shows that the turn-on voltage overshoot of a MOS-triggered SCR significantly depends on its gate voltage level.

Acknowledgements

The authors would like to gratefully thank E. Grund for mentoring this paper.

References

- [1] V. A. Vashchenko, et al, « Turn-off characteristics of the CMOS snapback ESD protection devices - new insights and its implications », in *EOS/ESD Symposium*, 2006, p. 39-45.

- [2] N. Thomson, et al « Exponential-edge transmission line pulsing for snap-back device characterization », in *IRPS*, 2013, p. 3E.2.1-3E.2.6.
- [3] T. Maloney and N. Khurana, « Transmission line pulsing techniques for circuit modeling of ESD phenomena », in *proc. EOS/ESD Symposium*, 1985, vol. 7, p. 49–54.
- [4] A. Delmas, et al, « Accurate transient behavior measurement of high-voltage ESD protections based on a very fast transmission-line pulse system », in *EOS/ESD Symposium*, 2009, p. 1-8.
- [5] H. Gieser and M. Haunschild, « Very-fast transmission line pulsing of integrated structures and the charged device model », in *Electrical Overstress/Electrostatic Discharge Symposium*, 1996. *Proceedings*, 1996, p. 85-94.
- [6] J. Willemen, A. Andreini, V. De Heyn, K. Esmark, M. Etheron, H. Gieser, G. Groeseneken, S. Mettler, E. Morena, N. Qu, W. Soppa, W. Stadler, R. Stella, W. Wilkening, H. Wolf, L. Zullino, « Characterization and modeling of transient device behavior under CDM ESD stress », in *Electrical Overstress/Electrostatic Discharge Symposium*, 2003. *EOS/ESD '03.*, 2003, p. 1-10.
- [7] J. Li, S. Hyvonen, E. Rosenbaum, « Improved wafer-level VFTLP system and investigation of device turn-on effects », in *Electrical Overstress/Electrostatic Discharge Symposium*, 2004. *EOS/ESD '04.*, 2004, p. 1-7.
- [8] R. A. Ashton, « Extraction of time dependent data from time domain reflection transmission line pulse measurements [ESD protection design] », in *Proceedings of the ICMTS*, 2005, p. 239-244.
- [9] D. Trémouilles, et al, « Transient voltage overshoot in TLP testing - Real or artifact? », in *EOS/ESD Symposium*, 2005, p. 1-9.
- [10] H. Wolf, et al, « Transient analysis of ESD protection elements by time domain transmission using repetitive pulses », in *EOS/ESD Symposium*, 2006, p. 304-310.
- [11] J. Manouvrier, P. Fonteneau, C.-A. Legrand, P. Nouet, F. Azais, « Characterization of the transient behavior of gated/STI diodes and their associated BJT in the CDM time domain », in *29th Electrical Overstress/Electrostatic Discharge Symposium*, 2007, p. 3A.2-1-3A.2-10.
- [12] H. A. Gieser and H. Wolf, « Survey on Very Fast TLP and Ultra Fast Repetitive Pulsing for Characterization in the CDM-Domain », in *Reliability physics symposium 2007 proceedings*, p. 324 -333.
- [13] R. Gillon, et al, « The application of large-signal calibration techniques yields unprecedented insight during TLP and ESD testing », in *EOS/ESD Symposium*, 2009, p. 1-7.
- [14] D. Linten, et al, « Calibration of very fast TLP transients », in *EOS/ESD Symposium*, 2009, p. 1-6.
- [15] D. Johnsson, M. Mayerhofer, J. Willemen, U. Glaser, D. Pogany, E. Gornik, M. Stecher, « Avalanche Breakdown Delay in High-Voltage p-n Junctions Caused by Pre-Pulse Voltage From IEC 61000-4-2 ESD Generators », *Device and Materials Reliability*, *IEEE Transactions on*, vol. 9, n° 3, p. 413-418, 2009.
- [16] A. Delmas, « Étude transitoire du déclenchement de protections haute tension contre les décharges électrostatiques », PhD Thesis, Université de Toulouse, France, February 27th, 2013.
- [17] A. Bennia et al., « Deconvolution of causal pulse and transient data ». *IEEE Transactions on Instrumentation and Measurement*, Vol 79. NO 6:933-939, 1990.
- [18] B. Parruck, « Study and performance evaluation of two iterative frequency domain de-convolution techniques ». *IEEE Transactions on Instrumentation and Measurement*, IM-33, n° 4 :281-287, 1984.
- [19] H. Arbess, D. Tremouilles, M. Bafleur, « High-temperature operation MOS-IGBT power clamp for improved ESD protection in smart power SOI technology », in *Electrical Overstress/Electrostatic Discharge Symposium (EOS/ESD)*, 2011, p. 1 -8.
- [20] Slavica Malobabi, David F. Ellis, Javier A. Salcedo, Yuanzhong (Paul) Zhou, Jean-Jacques Hajjar, Juin J. Liou, « Gate Oxide Evaluation under Very Fast Transmission Line Pulse (VFTLP) CDM-Type Stress », *Proceedings of the 7th International Caribbean Conference on Devices, Circuits and Systems*, Mexico, Apr. 28-30, 2008